Acta Manilana 71 (2023), 97-109

ISSN: 0065-1370

Acta Manilana

journal homepage: https://actamanilana.ust.edu.ph/

An α-Glucosidase and Pancreatic Lipase Inhibitory Cytochalasan Derivative from the Dothideomycetes fungus, *Sparticola triseptata*

Katherine Yasmin M. Garcia[1,2], Joe Anthony H. Manzano[1,3], and Allan Patrick G. Macabeo[1*]

[1]*Laboratory for Organic Reactivity, Discovery, and Synthesis (LORDS), Research Center for the Natural and Applied Sciences, University of Santo Tomas, España Blvd., 1015 Manila, Philippines*

[2]*Department of Chemistry, College of Science, University of Santo Tomas, España Blvd., 1015 Manila, Philippines*

[3]*The Graduate School, University of Santo Tomas, España Blvd., 1015 Manila, Philippines*

Graphical Abstract

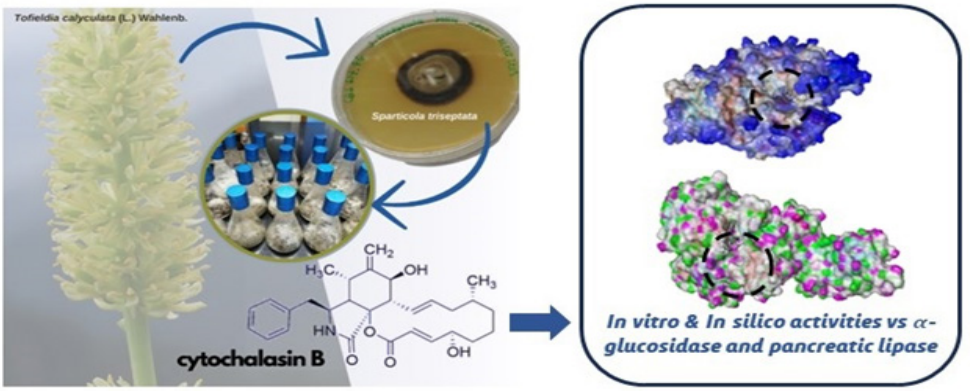

Abstract

The previously known cytotoxic cytochalasan, cytochalasin B (**1**), was isolated and purified from the ethyl acetate extract of the rice fermentation culture of the Alpine asphodel-associated Dothideomycetes fungus, *Sparticola triseptata* after iterative chromatographic purifications. The structure of **1** was established through extensive 1D and 2D-NMR spectroscopic experiments along with high-resolution electrospray ionization mass spectrometry (HRESIMS) and by comparison of its spectroscopic data with the literature. The potential of cytochalasin B (**1**) as antidiabetic and anti-obesity compound was screened using microplate, colorimetric enzyme inhibitory assays. Thus, **1** displayed significant *in vitro* α-glucosidase and porcine pancreatic lipase inhibitory activities with IC_{50} values of 5.46 µM and 8.43 µM, respectively when compared to the positive drug controls, acarbose and Orlistat®. Molecular simulation experiments using molecular docking showed moderately strong affinity of **1** onto the active sites of α-glucosidase and porcine pancreatic lipase with binding energies (BE) of -8.6 kcal/mol and -7.5 kcal/mol, respectively.

Keywords: Cytochalasan; cytochalasin B; Dothideomycetes; α-glucosidase; pancreatic lipase; molecular docking

Corresponding author: agmacabeo@ust.edu.ph

DOI: https://doi.org/10.53603/actamanil.71.2023.adzs2369

Date Received: 02 October 2023

Date Accepted: 15 November 2023

Introduction

Diabetes and obesity represent two of the most complex metabolic disorders that pose a significant challenge to public health worldwide. The prevalence of these chronic diseases has shown substantial increase over the past decades and have been recognized as an epidemic by the World Health Organization (WHO) [1]. According to WHO in 2019, diabetes caused 1.5 million deaths. Of these, 13% of adults aged 18 suffered obesity and diabetes.

A bidirectional relationship between these conditions has also been established, resulting in various metabolic complications [2]. Obesity is a well-known risk factor for type 2 diabetes as it causes insulin resistance, which disrupts glucose homeostasis. Diabetes, on the other hand, can aggravate obesity since insulin insufficiency or resistance can affect lipid metabolism and promote weight gain [3]. Therefore, novel avenues in natural products-derived therapeutics targeting these two metabolic disorders have been explored. Among the initial approaches for discovering new agents against diabetes and obesity are inhibitors of the enzymes α-glucosidase and lipases. Relevant to our study, a limited number of fungal-derived secondary metabolites from different taxa have been illustrated to exhibit inhibition against these two enzymes [4].

The Dothideomycetes, one of the largest fungal classes of Ascomycota, produces a spectrum of secondary metabolites that display structural complexity and a number of biological properties. Our initial efforts on the discovery of structurally unique secondary metabolites from the newly introduced genus *Sparticola* Phukhamsakda, Ariyawansa, Camporesi, & K.D. Hyde, ***gen. nov.*** [5-7] in particular the synonymized ascomycete soil-fungus from the decaying branches of the perennial herb, *Tofieldia calyculata* (L.) Wahlenb with *Massariosphaeria triseptate* (Lophiostomataceae), *S. triseptata* Phukhamsakda, Camporesi & K.D. Hyde, ***sp. nov.*** (family Sporormiaceae), led to the identification of unprecedented rearranged cytochalasin derivatives with antimicrobial, antiproliferative, and cytotoxic properties [8]. Cytochalasins possess a diverse spectrum of promising biological activities, including antimicrobial, antiviral, and antiparasitic properties [9–13], modulation of cytoskeletal growth, cellular motility, disruption of cytokinesis [14–15], regulation of hormonal functions [16–17], inhibition of cholesterol synthesis [18] and bacterial biofilms [19], interference with the glucose transport system [19–20], and intracellular Ca^{2+} regulation [21–22]. In this paper, we describe the isolation and identification of cytochalasin B from the solid rice culture of *S. triseptata*. As part of our growing interest to discover new antidiabetic and anti-obesity natural scaffolds [23-24], the enzyme inhibitory activities of cytochalasin B (**1**) against α-glucosidase and porcine pancreatic lipase were also explored *in vitro* and *in silico*.

Materials and Methods

General Experimental Procedures. Specific optical rotations ($[\alpha]_D$) were measured on a Perkin Elmer 241 polarimeter in a 100 mm × 2 mm cell at 20 °C. Nuclear magnetic resonance (NMR) spectroscopic data were acquired on an Agilent DD2 MR Varian-500 MHz (^{1}H 500 MHz, ^{13}C 125 MHz) and were obtained at 25 °C in MeOH-d_4, with reference to residual ^{1}H or ^{13}C signals of the deuterated solvent.

HR-ESI mass spectrum of **1** was measured using Agilent 6200 series TOF and 6500 series Q-TOF LC/MS system. HPLC-DAD purification of fungal fractions was performed on a Shimadzu Prominence Liquid Chromatograph LC-20AT coupled with SPD-M20A Photodiode Array Detector (Shimadzu Corp., Tokyo, Japan) using semi-preparative reversed-phase C18 column, Inertsil ODS-3 (10 mm I.D. x 250 mm, 5 µm, G.L. Sciences, Tokyo, Japan) as stationary phase. The mobile phase was composed of ultrapure water (Milli-Q, Millipore, Schwalbach, Germany) as solvent A and acetonitrile (HPLC grade) as solvent B.

Fungal Material. The ascomycete *Sparticola triseptata* (Leuchtm.) Phukhamsakda & K.D. Hyde, representing an ex-type strain of the species, was previously isolated from a decayed branch of *Tofielda calyculata* (L.) Wahlenb., and its morphological characters have previously been described by Leuchtmann et al. [27]. Based on a polyphasic taxonomic investigation that incorporated molecular phylogenetic and morphological approaches, this species was recently reassigned to the genus *Sparticola* by Phukhamsakda et al. [28]. The ex-type living culture is deposited at the KNAW Westerdijk Fungal Biodiversity Centre, Utrecht, the Netherlands (CBS 614.86).

Fermentation, Extraction, Isolation, and Structure Characterization. The fungus was cultured on malt extract agar plates for 8 – 10 weeks until the culture developed a characteristic brownish pigmentation. Five agar blocks of well-grown fungal culture were sub-cultured on a solid rice media (70 g brown rice, 0.3 g peptone, 0.1 g corn syrup, and 100 mL ultrapure water) in 15 x 1000 mL sterilized Fernbach culture flasks, followed by autoclaving (121 °C, 20 min) and incubated under static conditions at 25–30 °C for 12 weeks until the fungal hyphae have proliferated and the rice medium turning black in color. Fermentation was terminated by the addition of ethyl acetate (EtOAc) (3 x 300 mL). The combined extracts were concentrated on a rotary evaporator to afford the crude extract (30 g). The crude EtOAc extract was reconstituted with 300 mL 10% aqueous methanol and extracted with *n*-heptane (3 x 100 mL). The combined organic layer was concentrated *in vacuo* to afford a dark brown methanolic crude extract (8.8 g).

The methanolic crude extract was fractionated using silica gel column chromatography and elution was carried out using the following solvent systems: petroleum ether-EtOAc (1:1, 2:3, 3:7, 1:4, 1:9), EtOAc, dichloromethane (DCM), DCM-MeOH (9:1, 1:4, 7:3, 3:2, 1:1) and methanol to afford five combined main fractions. Fraction 3 (3.40 g) was chromatographed with DCM-MeOH (5:1) yielding three subfractions. The second subfraction (3.29 g) was subsequently eluted with DCM-MeOH (40:1) affording five subfractions. Fraction 3.2.1 (1.54 g) was further resolved using petroleum ether-EtOAc (2:1, 1:1) and DCM-MeOH (100:1, 80:1) to yield three pooled subfractions. The last subfraction, Fraction 3.2.1.3 (889 mg) was subjected to semi-preparative reversed phase HPLC using the following gradient system: 40% solvent B for 5 min, 40% – 100% solvent B for 20 min, 100% solvent B for 5 min and 100% – 40% solvent B for 5 min resulting to 10 fractions. Fraction 3.2.1.3.5 (53.8 mg) was purified twice using similar gradient conditions to yield compound **1** (6.87 mg, flow rate = 4.0 mL min−1, UV detection 200−600 nm, t_R = 22.85 min).

Cytochalasin B (**1**): white flakes; [α]D^{25} +30 (*c* 0.1, MeOH); TLC (CH_2Cl_2:MeOH, 9:1 v/v): R_f = 0.46; UV (*c* 0.1, MeOH) λ_{max} (log Ɛ) 208 (3.69), 213 (3.72), 229 (3.74) nm; ^1H and ^{13}C NMR data, Table 1; IR (KBr): 3555, 3283, 3250, 2865, 2840, 2450, 1720, 1700, 1635, 1600, 1455, 1270, 1090, 1035 cm^{-1}. HR-ESI-MS *m/z*: $[M + H]^+$ calcd for $C_{29}H_{38}NO_5$, 480.2750; found, 480.2745; *m/z* $[M + Na]^+$ calcd for $C_{29}H_{37}NaNO_5$, 502.2569; found, 502.2562.

α-Glucosidase Assay. The substrate *p*-nitrophenyl α-glucopyranoside (p-NPG) and α-glucosidase were purchased from Sigma, USA. Acarbose was used as positive control. The α-glucosidase inhibitory assay was performed by following the standard protocol with minor modifications [29-30]. Six various concentrations of 1, 10, 100. 250, 500, and 1000 µg/mL were prepared for compound **1**. The glucosidase assay was carried out by incubating the mixture containing 8 µL test compound, 112 µL NaH_2PO_4-Na_2HPO_4 buffer (pH 6.8) and, 20 µL glucosidase solution (0.2 U/mL) at 37 °C for 15 minutes. Initial absorbance was measured at 405 nm. After which, a volume of 20 µL of 2.5 mM *p*-NPG was added and the mixture was incubated for another 15 minutes at 37 °C. The reaction was halted by the addition of 80 µL 0.2 M Na_2CO_3 solution. The final absorbance of the reaction mixture was measured at 405 nm. The enzymatic hydrolysis of *p*-nitrophenyl glucopyranoside to *p*-nitrophenol was assessed thru the change in the absorption at 405 nm according to the formula:

$$Glucosidase\ inhibition\ (\%) = \left[\left(1 - \frac{\Delta ABS_{test\ compound}}{\Delta ABS_{\ control\ test} - \Delta ABS_{\ control\ blank}}\right) x\ 100\right]$$

The glucosidase inhibitory activity of each test compounds was plotted against the logarithmic concentrations and the IC_{50} values were reported.

Pancreatic Lipase Assay. The lipase inhibitory activity of compound **1** was identified using a colorimetric assay that quantifies the release of *p*-nitrophenol butyrate (*p*-NPB) as previously described in the protocol with slight modifications [31–32]. Orlistat® was used as positive control. A stock solution of 1 mg/mL test compounds in DMSO were used from which four different working solutions with the following concentrations of 0.1, 1.0, 10, and 100 µg/mL were prepared. The lipase enzyme solution was freshly prepared by dissolving 1 mg porcine pancreatic lipase in 1 mL Tris-HCl buffer (25 mmol Tris, pH=7.4 and 25 mmol NaCl). Lipase assay was performed in triplicate measurements by pre-incubating the mixture containing 20 µL of each test compound, 10 µL of pancreatic lipase enzyme, and 70 µL Tris-HCl buffer in a 96-well microtiter plate at 25 °C for 15 minutes. The enzymatic hydrolysis was started upon the addition of 15 µL *p*-NPB, which was then incubated at 37 °C for 30 minutes. The amount of *p*-nitrophenolate ions generated by the reaction was monitored by measuring the absorbance at 405 nm using a Glomax microplate reader.

Orlistat and DMSO were used as the positive and negative control, respectively, and the lipase activity was also evaluated with and without inhibitor by using the following formula:

$$Lipase\ inhibition\ (\%) = \left[100 - \left(\frac{B-b}{A-a}\ x\ 100\right)\right]$$

where A is the activity without inhibitor, a is the negative control without inhibitor, B is the activity with an inhibitor and b is the negative control with an inhibitor.

IC_{50} values of compound **1** were calculated using the least-squares regression line of the plots of the logarithm of the sample concentration (log) versus the pancreatic lipase inhibitory activity (%).

Molecular docking simulations. To prepare cytochalasin B (**1**) as a ligand, its SMILES notation was inputted in Avogadro (version 1.20), processed via geometry optimization, and saved as mol2 file. Protein targets like α-glucosidase and porcine pancreatic lipase were obtained from the Protein Data Bank using their PDB IDs 5ZCC and 1ETH, respectively. Both proteins were prepared and minimized in UCSF Chimera (version 1.16) using the steepest descent method with 100 steps (0.02 Å step size) [29–30]. The actual docking protocol followed the "flexible ligand into the flexible active site" using a generated grid in accordance with the Gasteiger charge method. Interactions were visualized in BIOVIA Discovery Studio (version 4.1) [33–34].

Results and Discussion

The EtOAc crude extract of *Sparticola triseptata* from the large-scale rice fermentation culture was partitioned between *n*-heptane and 10% aqueous MeOH. The resulting aqueous methanolic crude extract was fractionated and purified using silica gel column chromatography and semi-preparative HPLC to afford the previously known cytotoxic compound, cytochalasin B (**1**). The structure of **1** was identified based on its 1D and 2D NMR spectroscopic data, HRESIMS spectrum, and by comparing its spectroscopic data with the literature [35].

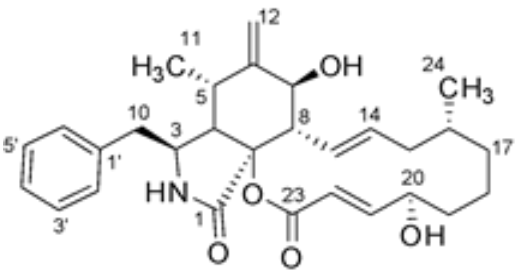

1

Figure 1. Structure of Cytochalasin B

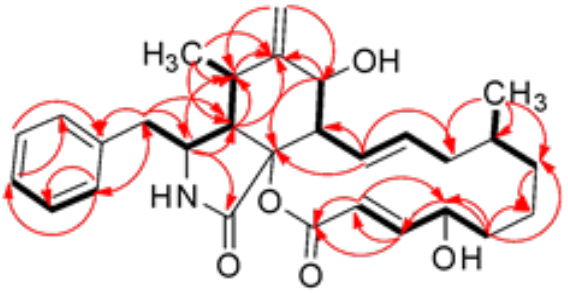

1

Figure 2. COSY (bold lines) and HSQC (red arrows) correlations of cytochalasin B

Compound **1** was obtained as optically active, white needles. The molecular formula $C_{29}H_{37}NO_5$ was deduced from its positive-ion HRESIMS data based on a protonated molecular ion $[M + H]^+$ detected at *m/z* 480.2745 (calcd 480.2750), implying 12 degrees of unsaturation. Detailed analysis of its ^{1}H, ^{13}C, and HSQC-DEPT spectroscopic data revealed 29 carbon signals (with two carbon signals overlapping with MeOH-d_4) corresponding to two carbonyl carbons, three quaternary carbons (two sp^2 and one sp^3), five aromatic methines, four olefinic methines, seven sp^3 methines (two oxygenated and five non-oxygenated), five methylene carbons, one exomethylene carbon, and two methyl carbons. Interpretation of the 1D NMR spectra allowed the identification of a cytochalasin core and supported by 2D NMR spectroscopic data (Table 1).

The perhydro-isoindolone moiety was identified via HMBC correlations primarily from the resonance signals of H–3 (δ_H 3.32) to C–1 (δ_C 173.9) and C–4 (δ_C 48.5), from H–4 (δ_H 2.85) to C–5 (δ_C 32.9), C–6 (δ_C 151.4) and C–9 (δ_C 85.4), H_3–11 (δ_H 0.85) to C–4, C–5 and C–6, from H_2–12 (δ_H 5.08, 5.28) to C–5 and C–7 (δ_C 71.5), from H–8 (δ_H 3.32) to C–1 and C–9 (δ_C 85.4). In the COSY spectrum, a three-distinct spin system displaying cross peaks of H–2′/H–6′ (δ_H 7.13) and H–3′/H–5′ (δ_H 7.26), and of H–4′ (δ H 7.18) corresponding to C–2′/C–6′ (δ_C 131.0) to C–4′ (δ_C 127.8), along with the HMBC correlations from H–2′/H–6′ to C–10, and from H_2–10 (δ_H 2.82) to C–1 and C–2′/C–6′ led to the attachment of the phenyl moiety to the perhydro-isoindolyl subunit. The remaining part of **1** was determined to be a 13-membered macrocyclic ring which was supported by the five-proton spin system resonating from H–7 → H–8 → H–13 → H–14 → H_2–15, three-proton spin system from H–24 → H–16 → H–17 and additional four distinct spin system from H–19 → H–20 → H–21 → H–22 (Figure 2). Finally, HMBC correlations from H–13 (δ_H 5.83) to C–8 (δ_C 49.2), C–7 (δ_C 71.5), and C–9 (δ_C 85.4), as well as resonances from H–22 (δ_H 5.77) to C–23 (δ_C 166.4) and C–9 suggested the connectivity of the 13-membered macrocyclic ring residue to the 10-phenylperhydro-isoindolone moiety. Based on HMBC correlations and corroboration with homonuclear COSY experiments, the proton and carbon signals of the cytochalasin core and the macrocyclic ring fragment were noted to be characteristic of cytochalasin B. Comparison of the ^{1}H and ^{13}C NMR spectroscopic data of **1** and cytochalasin B indicated similar resonance signals [36].

Table 1. NMR spectroscopic data of **1** in MeOH-d_4.

position	δ_C [a]	**1** δ_H [b] (*J* in Hz)	HMBC
1	173.9, C	-	
3	54.8, CH	3.32, m (1H)	
4	48.5, CH	2.85, m (1H)	
5	32.9, C	3.19, m	3, 4, 5, 7
6	151.4, C	-	2, 3, 4, 5, 7
7	71.5, CH	3.79, d (10.9, 1H)	1, 3, 4, 5, 7
8	49.2, CH	3.32, m (1H)	9, 1, 10
9	85.4, C	-	
10a	44.1, CH_2	2.82, m (2H)	
10b			
11	14.1, CH_3	0.85, d (6.6, 3H)	
12a	114.3, CH_3	5.08, br s (1H)	11, 13, 15, 20
12b		5.28, br s (1H)	
13	128.7, CH	5.83, ddd (15.0, 9.8, 1.7, 1H)	11, 15, 20
14	136.7, CH	5.23, ddd (15.0, 3.6, 1.7, 1H)	11, 12, 13, 15
15a	35.4, CH_2	1.58 – 1.52, m (1H)	
15b		1.90, ddd (14.1, 4.0, 2.2, 1H)	
16	34.5, CH	1.23, m (1H)	19, 18, 17, 15
17a	36.6, CH_2	0.57, m (1H)	
17b		1.71, m (1H)	19, 15, 20
18a	21.5, CH_2	1.31 – 1.27 (m, 1H)	19, 17, 15, 20
18b		1.48 – 1.41 (m, 1H)	
19a	43.2, CH_2	1.65, m (1H)	
19b		2.08, m (1H)	
20	71.2, CH	4.43, m (1H)	
21	154.7, CH	6.92, dd (15.7, 4.5, 1H)	
22	119.5, CH	5.77, dd (15.7, 1.8, 1H)	
23	166.4, C	-	
24	20.7, CH_3	0.87, d (6.8 Hz, 3H),	
1′	138.3, C	-	
2′/6′	131.0, CH	7.13, d (7.4, 2H)	
3′/5′	129.6, CH	7.26, dd (7.4, 7.4 2H)	
4′	127.8, CH	7.18, dd (7.4, 7.4, 1H)	

[a]Recorded at 150 MHz, [b]Recorded at 600 MHz; Carbon multiplicities were deduced from HSQC-DEPT-135 spectra; [c]HMBC correlations, optimized for 10 Hz, are from the proton(s) stated to the indicated carbon(s).

Diabetes mellitus is a chronic metabolic disorder characterized by elevated blood glucose levels, which results either from insufficient or impaired insulin production. The rapid absorption of glucose from dietary carbohydrates is one of the primary causes of postprandial hyperglycemia. In the small intestine, α-glucosidase facilitates the digestion of complex sugars. These enzymes hydrolyze glycosidic bonds in carbohydrates to release glucose for absorption. As a result, α-glucosidase activity significantly influences the rate at which glucose enters the bloodstream. Thus, α-glucosidase inhibitors have emerged as a novel medicinal strategy to mitigate postprandial hyperglycemia by lowering the enzymatic activity that could lead to delayed carbohydrate breakdown and allow a more gradual release of glucose into the bloodstream [37]. Currently, a number of pharmaceutical drugs, namely sulfonylureas, biguanides, and thiazolidinediones are used in the management of this disease [38].

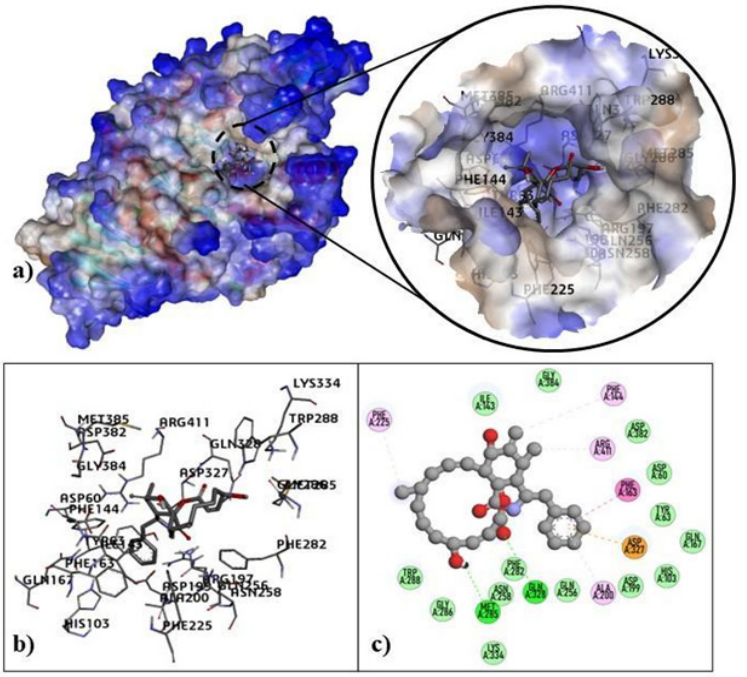

Figure 3. (a) Dock pose and (b, c) interactions of cytochalasin B (**1**) in the active site of α-glucosidase.

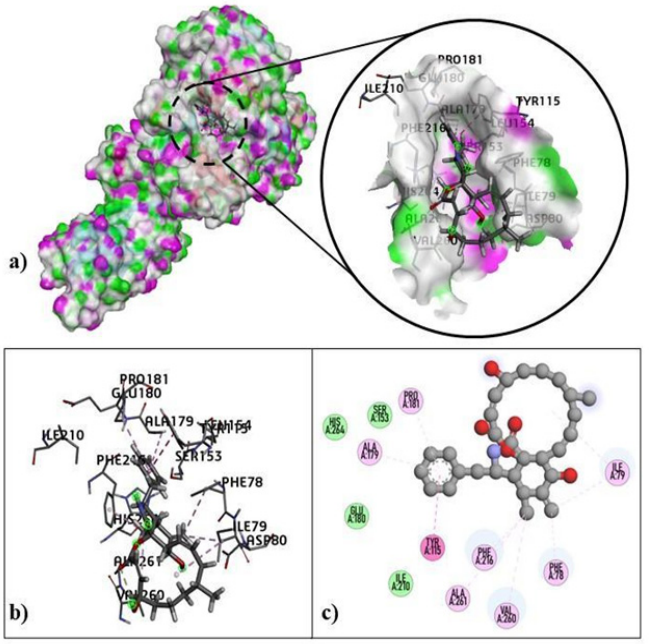

Figure 4. (a) Dock pose and (b, c) interactions of cytochalasin B (**1**) in the active site of porcine pancreatic lipase.

Table 2. In vitro (expressed as IC_{50}) and in silico (expressed as binding energies or BE) inhibitory activities of cytochalasin B (1), and positive controls vs target enzymes α-glucosidase and pancreatic lipase.

Test compounds	IC_{50} vs α-glucosidase (μM)	BE vs α-glucosidase (kcal/mol)	Interactions	IC_{50} vs pancreatic lipase (μM)	BE vs PPL (kcal/mol)	Interactions
Cytochalasin B (**1**)	5.46	-8.6	Gln328, Met285 (H-bond), Asp327 (π-anion), Phe163 (π- π), Ala200, Phe225, Phe144, Arg411 (alkyl / π-alkyl)	8.43	-7.5	Tyr115 (π-π), Ile79, Phe78, Val260, Phe216, Ala261, Ala179, Pro181 (alkyl / π-alkyl)
Acarbose	3.36	-8.5	His203, Asp382, Ser145, Ser142, Glu141, Asp327 (H-bond), Asp327 (attractive charge), Ile143, Thr409, Gln256, Glu141 (C-H bond / π-donor bond)	-	-	-
Orlistat	-	-	-	5.49	-7.3	His264, Phe78, Ser153 (H-bond), Asp80 (attractive charge), Phe216 (π-σ), Leu265, Tyr115, Pro181, Val260, Arg257, Trp253, Ile79, Ala261 (alkyl / π-alkyl)

(-) = not determined / not applicable; IC_{50} values are represented as mean based on triplicate measurement;
PPL = porcine pancreatic lipase; BE = binding energy.

However, a number of undesirable gastrointestinal side effects have been reported. In our study, compound **1** was screened for in vitro inhibition of α-glucosidase and resulted to a strong inhibition (IC_{50} = 5.46 μM) with comparable results to the positive control, acarbose (IC_{50} = 3.36 μM) (Table 2).

Cytochalasin B (**1**) was also assessed for its inhibitory activity against pancreatic lipase, a hydrolase responsible for the breakdown of complex triacylglycerides to free fatty acids and monoacylglycerol for absorption. Targeting this enzyme may present a therapeutic approach for the management of obesity since it regulates triacylglycerol absorption and consequently prevents associated-metabolic complications [39]. Cytochalasan **1** demonstrated strong inhibition of porcine pancreatic lipase (IC_{50} = 8.43 μM). The reference drug control Orlistat® showed an IC_{50} of 5.49 μM (Table 2). Our *in vitro* enzyme inhibition data show potential for cytochalasin B against α-glucosidase and pancreatic lipase for designing compounds that may control blood glucose levels and obesity.

To probe the putative binding mechanisms and modalities of cytochalasin B (**1**), molecular docking experiments against α-glucosidase and pancreatic lipase were conducted. Congruent to the *in vitro* results, compound **1** showed comparable binding affinity to α-glucosidase (BE = - 8.6 kcal/mol) with the positive control acarbose (BE = - 8.5 kcal/mol) (Table 2; Figure 3a). It formed H-bond with Gln328 and Met 285; π-anion with Asp327; and alkyl or π-alkyl interactions with Ala200, Phe225, Phe144, and Arg411. Interestingly, amino acid Asp327 was both targeted by 1 and acarbose (Table 2; Figure 3b-c). Docking results with porcine pancreatic lipase (PPL) illustrated almost similar binding propensities for 1 (BE = - 7.5 kcal/mol) and positive control Orlistat® (BE = -7.3 kcal/mol) (Table 2; Figure 4a). Compound **1** was bound to the active site of PPL via π-π interaction with Tyr115; and alkyl or π-alkyl interactions with Ile79, Phe78, Val260, Phe216, Ala261, Ala179, and Pro181.

Phe78, Phe216, Pro181, Val260, Ala261, and Ile79 were the common target residues of both **1** and Orlistat® (Table 2; Figure 4b-c). In general, results of molecular docking simulations are considered significant in drug discovery due to identification of important target amino residues. Specific chemical moieties which may bind or repel residues in the active site may reveal structural specificity and thus provide details in designing new generation of natural product-based drug pharmacophores against diabetes- and obesity-implicated enzymes [30, 40-42].

Conclusion

The known cytochalasan derivative **1** was isolated and identified from the MeOH sub-extract of the Sporormiaceous species *Sparticola triseptata*. Its structure was confirmed using extensive spectroscopic experiments and by comparison with the literature. Cytochalasin B exhibited *in vitro* and *in silico* inhibitions against α-glucosidase and porcine pancreatic lipase demonstrating its potential to be developed as antidiabetic and anti-obesity agent.

Acknowledgment

KYMG acknowledges the Department of Science and Technology (DOST) thru its Accelerated Science & Technology Human Resource Development Program (ASTHRDP).

Conflict of Interest

The authors declare no conflict of interest.

Author Contributions

Conceptualization, methodology, data collection analysis and interpretation of data, original draft preparation, review and editing of the draft, K.Y.M.G., J. A. H. M. and A.P.G.M. Methodology, data collection analysis and interpretation of data, review and editing of the draft, K.Y.M.G., J. A. H. M.. All authors have read and agreed to the final version of the manuscript.

Funding

Department of Science and Technology (DOST)/Accelerated Science & Technology Human Resource Development Program (ASTHRDP).

Institutional Review Board Statement

Not applicable.

Informed Consent Statement

Not applicable.

References

[1] Chobot A, Górowska-Kowolik K, Sokołowska M, & Jarosz-Chobot P. Obesity and diabetes-Not only a simple link between two epidemics. Diabetes/Metabolism Research and Reviews **2018**; 34(7), 3042–50.

[2] Grant B, Sandelson M, Agyemang-Prempeh B, & Zalin A. Managing obesity in people with type 2 diabetes. Clinical Medicine **2021**; 21(4), 327–31.

[3] Padhi S, Nayak AK, & Behera A. Type II diabetes mellitus: a review on recent drug-based therapeutics. Biomedicine & Pharmacotherapy **2020**;131, 1107–08.

[4] Hyde KD, Xu J, Rapior S, Jeewon R, Lumyong S, et al. The amazing potential of fungi: 50 ways we can exploit fungi industrially. Fungal Divers **2019**; 97(1), 1–136.

[5] Phukhamsakda C, Macabeo APG, Cheng T, Huch V, Hyde KD, Stadler M. Sparticolins A–G, biologically active spirodioxynapthalene derivatives from the ascomycocete *Sparticola junci*. Journal of Natural Products **2019**; 82 (10), 2878–85.

[6] Garcia KYM, Quimque MTJ, Primahana G, Ratzenböck A, Cano MJB, Llaguno JFA, Dahse H-M, Phukhamsakda C, Surup F, Stadler M, Macabeo APG. COX Inhibitory and Cytotoxic Naphthoketal-Bearing Polyketides from *Sparticola junci*. International Journal of Molecular Sciences **2021**; 22(22), 12379–91.

[7] Garcia KYM, Phukhamsakda C, Quimque MTJ, Hyde KD, Stadler, A. P. G. Macabeo APG. Catechol-bearing polyketide derivatives from *Sparticola junci*. Journal of Natural Products **2021**; 84(7), 2053–58.

[8] Garcia KYM, Quimque MTJ, Lambert C, Schmidt K, Primahana G, et al. Antiproliferative and cytotoxic cytochalasins from *Sparticola triseptata* inhibit actin polymerization and aggregation. Journal of Fungi **2022**; 8(6), 560–73.

[9] Betina V, Micekova D, & Nemec P. Antimicrobial properties of cytochalasins and their alteration of fungal morphology. Journal of General Microbiology **1972**; 71, 343–49.

[10] Horn WS, Simmonds MSJ, & Blaney WM. Phomopsichalasin, a novel antimicrobial agent from an endophytic *Phomopsis* sp. Tetrahedron **1995**; 51, 3969–78.

[11] Makioka A, Kumagai M, Kobayashi S, & Takeuchi T. Effect of proteasome inhibitors on the growth, encystation, and excystation of *Entamoeba histolytica* and *Entamoeba invadens*. Parasitology Research **2004**; 93, 68–71.

[12] Jayasuriya H, Herath KB, Ondeyka JG, Polishook JD, Bills GF, et al. Isolation structure of antagonists of chemokine receptor (CCR5). Journal of Natural Products **2004**; 67, 1036–38.

[13] Rochfort S, Ford J, Ovenden S, Wan SS, George S, et al. A novel aspochalasin with HIV-1 integrase inhibitory activity from *Aspergillus flavipes*. Journal of Antibiotics **2005**; 58, 279–83.

[14] Scherlach K, Boettger D, Remme N, & Hertweck C. The chemistry and biology of cytochalasans. Natural Product Reports **2010**; 27, 869–86.

[15] Kretz R, Wendt L, Wongkanoun S, Luangsa-ard JJ, Surup F, et al. The effect of cytochalasans on the actin cytoskeleton of eukaryotic cells and preliminary structure–activity relationships. Biomolecules **2019**; 9, 73–86.

[16] Schofield JG. Cytochalasin B and release of growth hormone. Nature: New Biology **1971**; 234(50), 215–6.

[17] Williams JA, & Wolff J. Cytochalasin B inhibits thyroid secretion. Biochemical and Biophysical Research Communications **1971**; 44, 422–5.

[18] Crivello JF, & Jefcoate CR. Intracellular movement of cholesterol in rat adrenal cells. Kinetics and effects of inhibitors. Journal of Biological Chemistry **1980**; 255, 8144–51.

[19] Yuyama KT, Wendt L, Surup F, Chepkirui C, Wittstein K, et al. Cytochalasans act as inhibitors of biofilm formation of *Staphylococcus aureus*. Biomolecules **2018**; 8, 129–41

[20] Rampal AL, Pinkofsky HB, & Jung CY. Structure of cytochalasins and cytochalasin B binding sites in human erythrocyte membranes. Biochemistry **1980**; 19, 679–83.

[21] George TP, Cook HW, Byers DM, Palmer FBSC, & Spence MW. Inhibition of phosphatidylcholine and phosphatidylethanolamine biosynthesis by cytochalasin B in cultured glioma cells: Potential regulation of biosynthesis by Ca^{2+}-dependent mechanisms. Biochimica et Biophysica Acta **1991**; 1084, 185–93.

[22] Ebstensen RD, & Plagemann PG. Cytochalasin B: inhibition of glucose and glucosamine transport. Proceedings of the National Academy of Sciences of the United States of America, **1972**; 69(6), 1430–34.

[23] Macabeo AP, Pilapil LA, Garcia KY, Quimque MT, Phukhamsakda C, Cruz AJ, Hyde KD, & Stadler M. Alpha-glucosidase-and lipase-inhibitory phenalenones from a new species of *Pseudolophiostoma* originating from Thailand. Molecules, **2020**; 25(4), 965–73.

[24] Macabeo APG, Rubio PYM, Alejandro GJD, & Knorn M. An α-glucosidase inhibitor from *Drepananthus philippinensis*. Procedia Chemistry, **2015**; 14, 36–9.

[25] Macabeo AP, Cruz AJ, Narmani A, Arzanlou M, Babai-Ahari A, Pilapil LA, Garcia KY, Huch V, & Stadler M. Tetrasubstituted α-pyrone derivatives from the endophytic fungus, *Neurospora udagawae*. Phytochemistry Letters, **2020**; 35, 147–51.

[26] Quimque MT, Magsipoc RJ, Llames LC, Flores AI, Garcia KY, Ratzenböck A, Hussain H, & Macabeo AP. Polyoxygenated Cyclohexenes from *Uvaria grandiflora* with Multi-Enzyme Targeting Properties Relevant in Type 2 Diabetes and Obesity. ACS Omega, **2022,** 7(41), 36856–64.

[27] Leuchtmann A. *Phaeosphaera padellana* und *Massariosphaeria triseptata*, zwei neue bitunicate Ascomyceten aus den Alpen. Mycologia Helvetica **1987**; 2, 183–91.

[28] Phukhamsakda C, Ariyansawa HA, Phillips AJL, Wanasinghe DN, Bhat DJ, et al. Additions to sporormiaceae: Introducing two novel genera, *Sparticola* and *Forliomyces*, from Spartium. Cryptogamie Mycologie **2016**; 37, 75–97.

[29] Li Y, Li C, Xu Q, & Kang W. Antioxidant, α-glucosidase inhibitory activities in vitro and alloxan-induced diabetic rats' protective effect of *Indigofera stachyodes* Lindl. root. Journal of Medicinal Plants Research **2012**; 6, 1524–31.

[30] Manzano JAH, Llames LCJ, & Macabeo APG. Tetrahydrobisbenzylisoquinoline alkaloids from *Phaeanthus ophthalmicus* inhibit target enzymes associated with type 2 diabetes and obesity. Journal of Applied Pharmaceutical Science **2023**. http://doi.org/10.7324/JAPS.2023.154518.

[31] Jaradat N, Zaid A, Hussein F, Zaqzouq M, Aljammal H, & Ayesh O. Anti-lipase potential of the organic and aqueous extracts of ten traditional edible and medicinal plants in Palestine: A comparison study with Orlistat. Medicines **2017**; 4(4), 89–101.

[32] Malaluan IN, Manzano JA, Muñoz JE, Bautista TJ, Dahse HM, Quimque MT, & Macabeo APG. Antituberculosis and antiproliferative activities of the extracts and tetrahydrobisbenzylisoquinoline alkaloids from *Phaeanthus ophthalmicus*: *in vitro* and *in silico* investigations. Philippine Journal of Science **2022**; 151(1), 371–81.

[33] Manzano JA, III CL, Quimque MT, & Macabeo AP. In silico potentials of *Alpinia galanga* constituents against human placental aromatase vital in postmenopausal estrogen-dependent breast cancer pathogenesis. Philippine Journal of Science **2022**; 151(6A), 2101–15.

[34] Wang J, Wang W, Kollman PA, & Case DA. Automatic atom type and bond type perception in molecular mechanical calculations. Journal of Molecular Graphics and Modelling **2006**; 25(2), 247–60.

[35] Pettersen EF, Goddard TD, Huang CC, Couch GS, Greenblatt DM, Meng EC, et al. UCSF Chimera—a visualization system for exploratory research and analysis. Journal of Computational Chemistry **2004**; 25(13), 1605–12.

[36] Capasso R, Evidente A, Randazzo G, Ritieni A, Bottalico A, et al. Isolation of cytochalasins A and B from *Ascochyta heteromorpha*. Journal of Natural Products **1987**; 50(5), 989–90.

[37] Patil P, Mandal S, Tomar SK, & Anand S. Food protein-derived bioactive peptides in management of type 2 diabetes. European Journal of Nutrition **2015**; 54, 863–80.

[38] Padhi S, Nayak AK, & Behera A. Type II diabetes mellitus: a review on recent drug-based therapeutics. Biomedicine & Pharmacotherapy **2020**; 131, 1107–08.

[39] Zhu G, Fang Q, Zhu F, Huang D, & Yang C. Structure and Function of Pancreatic Lipase-Related Protein 2 and Its Relationship with Pathological States. Frontiers in Genetics **2021**; 12, 6935–38.

[40] Jhong CH, Riyaphan J, Lin SH, Chia YC, & Weng CF. Screening alpha-glucosidase and alpha-amylase inhibitors from natural compounds by molecular docking *in silico*. Biofactors **2015**; 41(4), 242–51.

[41] Ahmed B, Ali Ashfaq U, & Usman Mirza, M. Medicinal plant phytochemicals and their inhibitory activities against pancreatic lipase: molecular docking combined with molecular dynamics simulation approach. Natural Product Research **2018**; 32(10), 1123–9.

[42] Liu JL, Kong YC, Miao JY, Mei XY, Wu SY, Yan YC, & Cao XY. Spectroscopy and molecular docking analysis reveal structural specificity of flavonoids in the inhibition of α-glucosidase activity. International Journal of Biological Macromolecules **2020**; 152, 981–9.